2022
9(1), 68-73

Journal of
MATERIALS NANOSCIENCE

Enhanced Room Temperature Selective Ammonia Sensing Based on SnO_2 Decorated MXene

Kamaraj Govindharaj,[1] Manoharan Mathankumar,[1] Krishnamoorthy Rajavel,[2] Yuvaraj Haldorai,[1] Ramasamy Thangavelu Rajendra Kumar[1*]

[1]*Advanced Materials and Devices Laboratory (AMDL), Department of Nanoscience and technology, Bharathiar University, Coimbatore 641 046, Tamil Nadu, India.* [2]*Shenzhen Institute of Advanced Electronic Materials, Shenzhen Institutes of Advanced Technology, Chinese Academy of Sciences, Shenzhen, 518055, China.*

Submitted on: 25-Nov-2021, Accepted and Published on: 15-Feb-2022

Article

ABSTRACT

Tin oxide (SnO_2)/MXene nanocomposites were prepared by decorating SnO_2 nanoparticles over two dimensional (2D) few-layer titanium carbide MXene ($Ti_3C_2T_x$) using ultra-sonication. The prepared SnO_2/MXene composite sensor device exhibited highly selective and sensitive detection towards trace level of ammonia gas molecules and the sensor device operated at room temperature with linear sensing response R^2=0.98987, and 0.98971 towards ammonia concentrations of 0.5 to 5 ppm and 10 to 100 ppm, respectively. Remarkably, the SnO_2 nanoparticles decorated MXene sheets showed shorter response time about 16 s compared to the pristine SnO_2 (61 s) and MXene (300 s). Besides, quick reversibility over multiple cycles, room temperature operation, high sensitivity, faster response/recovery time, and simple fabrication approach of making SnO_2 decorated MXene materials could be interesting for making next generation sensors for selective detection of ammonia.

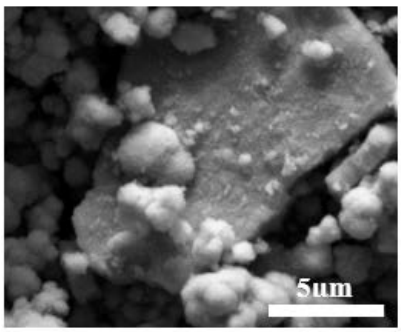

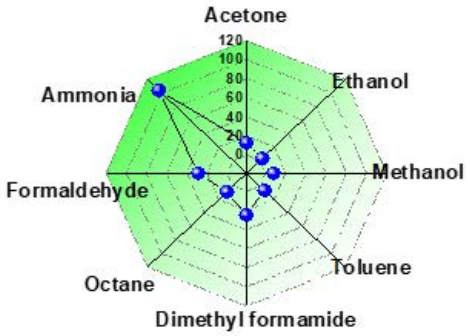

Keywords: MXene, SnO_2, Chemiresistive sensor, Nanoparticle, Heterojunction

INTRODUCTION

Ammonia is one of the highly used vapors in the various industries, such as leather field,[1] rubber,[2] waste water treatment[3] and fertilizer companies.[4] Inhalation of ammonia leads to severe carcinogenic effects to human body like, respirational problem, kidney diseases and skin allergies. The human threshold limits (TLV) to inhale ammonia gas is below 25 ppm (parts per million) and not more than 8 hours. Continuous exposure, even trace level of ammonia gas can create dangerous effects to living system specifically carcinogenic effect to human physiological system.[5] Therefore, development of cost-effective gas sensors capable of identifying low concentrations of ammonia molecules with excellent stability and sensitivity are required. In addition, that fabrication of gas sensor for continuous monitoring of toxic ammonia gas is highly desirable and most wanted technology in electronic and environmental monitoring applications. Currently, many metal oxide semiconducting nanostructures has been identified as an active material to detect ammonia (ZnO,[6–8] WO_3,[9,10] Fe_2O_3,[11,12] MoO_3[13,14]). Semiconducting materials requires high temperature for effective operations during gas molecule detection, thus the gas sensor assembly could be fitted with heating filaments. Substrate heaters consumes excessive voltage for the sensing so, it will increase the operational cost of the sensor.

Alternatively, carbon nanomaterials-based gas sensors were explored;[15] it does not require temperature for effective detection of the gas molecules even in trace level detection applications which showed fast response and recovery time.[16] Two dimensional (2D) layered materials possessed for practical applications in gas sensor fabrications.[17] Still interesting research progress required in 2D materials for reliable performance which could fit into the gas sensing characteristics to move forward in sensor technology for real time monitoring. Recently, the newly explored 2D transition metal carbides (MXene-$Ti_3C_2T_x$, where T_x

*Corresponding Author: Dr. R.T. RajendraKumar, Professor, Department of Nanoscience and Technology, School of Physical Sciences, Bharathiar University, Coimbatore - 641 046, India.
Tel: +91-9789757888 (M), +91-422-2428446, Fax: +91-422-2422387
Email: rtrkumar@buc.edu.in

URN:NBN:sciencein.jmns.2022.v9.299
 ISSN: 2394-0867
https://pubs.thesciencein.org/jmns

represents either -OH or -F groups are used for gas sensing application,[18] and these MXene was synthesized by aluminum etching off process from the MAX (Ti_3AlC_2) phase. Pristine metal carbides show considerable gas sensing response[19] however, have poor discriminating ability in mixed gas environment.[18] In order to overcome the short comings in pure MXene materials for gas sensor applications, different combinations with metal oxide semiconductor[20–22] have been projected. Generally, metal sulphide and selenide materials are good candidates for making heterojunction with MXene nanostructures. However, the toxic nature of sulphide and selenide limits their usage. Generally, most of the gas adsorption during gas sensing basically depends on number of adsorbed oxygen species and the active sites on the material surface. Ultimately, increasing number of adsorbed oxygen and active sites in sensor materials can also be attained by SnO_2 and MXene heterojunctions.[23,24] Therefore, the present study reported fabrication of electrostatically assembled SnO_2/MXene nanocomposites possessed with more number of heterojunctions and studied its gas sensing performance for the first time. According to our knowledge, synthesis of (SnO_2) semiconducting nanoparticles decorated on few-layered MXene ($Ti_3C_2T_x$) without altering its inherent properties of individual materials and its gas sensing properties has never been studied so far. The fabricated SnO_2/MXene materials displayed maximum allowable number of heterojunction favorable to superior gas sensing performance.[25] The gas sensing performance and selectivity towards ammonia molecules of synthesized SnO_2 decorated MXene were analyzed with different analytes molecules.

MATERIALS AND METHODS

Synthesis of $Ti_3C_2T_x$ and SnO_2

Few-layer MXene ($Ti_3C_2T_x$) was prepared by a minimal intensive layer delamination (MILD) method according to the previous report.[26] The selective etching off Al from Ti_3AlC_2 by using LiF and HCl could form 2D few-layers of MXene. The finally collected few layers suspension (inset of Figure 3b) with desired concentrations were used to prepare SnO_2/MXene nanocomposites.

For SnO_2 nanoparticle synthesis, 0.06 M stannous chloride hydrate was dissolved in 40 mL distilled water. The solution was continuously stirred for 15 min. Then, 4 mL of H_2SO_4 was added to the solution and stirred vigorously for 30 min before transferring into 100 mL Teflon-lined stainless-steel autoclave. The autoclave was heated at 200 °C for 24 h and cooled naturally to room temperature. After repeated washing and drying the desired SnO_2 nanoparticles were obtained.

Decoration of SnO_2 nanoparticles on MXene

The desired concentration of (5 mg/mL) of SnO_2 nanoparticles was mixed with MXene (20 µg) solution and then sonicated for 30 min to form electrostatic assembly of SnO_2/MXene nanocomposites (inset of Figure 3a). Individually, different concentrations (20, 40, 60, and 80 µg) of MXene were added into well dispersed SnO_2 solution (5 mg/mL) and subject for 30 min bath sonication to prepare different MXene decorated SnO_2 (5mg) nanoparticles. The obtained SnO_2/MXene nanocomposites were named accordingly as 5:20, 5:40, 5:60, and 5:80. From the above uniform suspension 5 µL was taken from the stock solutions and drop coated on the interdigitated silver electrode and dried at 70 ºC for 12 h.

Characterization

The pristine SnO_2, MXene and SnO_2/MXene nanocomposites were characterized using X-Ray diffraction analysis (XRD) using D/Max2550V, Rigaku, Japan. Morphological analysis of the prepared SnO_2/MXene nanocomposites were analysized using Field Emission Scanning Electron Microscope (FESEM) equipped with FEI Tecnai G230 together with elemental mapping and Energy-Dispersive X-Ray Spectroscopy spectrum (EDS).

Gas sensing measurement

The in-house fabricated gas sensing setup (Figure 1) was used for testing gas sensing performance of fabricated SnO_2/MXene nanocomposites samples. The sensor setup comprises of programmable mass flow controllers, bubblers, sensing chamber and computer connected electrical measuring unit as shown in Figure 1.

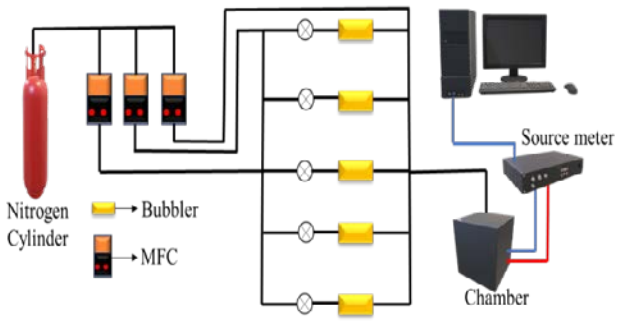

Figure 1. Schematics of the in-house fabricated gas sensing setup.

The nitrogen gas used as a dilution/carrier gas; ammonia liquid passed through the gas bubbler to generate different concentrations of vapor gas. Keysight B2912A precision source meter was connected to the computer to measure the change in resistance of the sensor upon gas interaction on the sensor surface.

RESULTS AND DISCUSSION

Structural and Morphological characterization

Figure 2 shows the XRD pattern of MXene, SnO_2 and SnO_2/MXene nanostructures. Initially, MXene was synthesized by selective removal of Al from MAX phase, we can clearly see the lower angle peak position around 9.93º indicated formation of 2D MXene layers which are aligned with previous reports.[27] For SnO_2, the major sharp peaks at 26.67º and 33.99º, confirming the high crystallinity of the material. The observed crystalline peak position of pristine SnO_2 was coinciding with ICDD no 01-080-6417 and it confirms the hexagonal structure of SnO_2.[28] Lattice parameter and crystallite size were calculated using Scherrer formula,[29]

$$D_p = \frac{K\lambda}{\beta\, Cos\theta}$$

where, D_p is the mean size of crystallites (nm), K is crystallite shape factor (0.9), λ is the X-ray wavelength, β is the full width at half the maximum (FWHM), and θ is the Braggs' angle (deg). The calculated average crystalline size is about 20.33 nm for the SnO_2/MXene nanocomposite samples. The measured Lattice parameter is about a =4.715 Å, b=4.715 Å, and c= 3.194 Å which correlated with previous reports on the synthesis of SnO_2 nanoparticles.[30] In the case of SnO_2/MXene nanocomposites, the XRD peaks associated with SnO_2 nanoparticles dominates over peaks associated with MXene due to minimum loading of MXene into SnO_2 suspension.

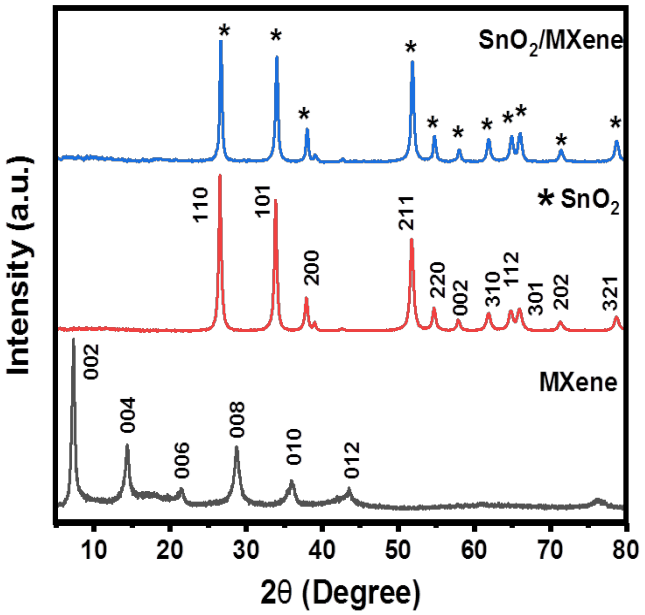

Figure 2. XRD spectra of MXene, SnO_2, and SnO_2/MXene.

The morphological features of prepared SnO_2, MXene and SnO_2/MXene nanocomposites were analyzed by FESEM and results are presented in Figure 3. It is evident from Figure3a that nearly spherical shaped SnO_2 nanoparticles of size ranged 10 to 30 nm and agglomerated together. Figure 3b shows FESEM images of the exfoliated few-layer MXene, the images were recorded in MXene free standing film[27] which shows that number of individual layers were stacked together after free standing film forming process. The FESEM images of prepared SnO_2/MXene are given in Figure 3 (c and d). As evidenced from the Figure 3(c and d), the aggregated SnO_2 nanoparticles were attached onto the MXene surface. The weak Van der Waals interaction between the SnO_2 leads to the agglomerated larger sized SnO_2 particles. The photographic image of pure SnO_2 nanoparticles (inset image of Figure 3a) dispersed in distilled water (5:1 ratio) shows clear dispersion of nanoparticles in water medium. In our experimental conditions, all three liquid phase samples were clearly showed transparent to the laser light confirms that, all samples were uniformly dispersed. Further, elemental mapping and EDS spectrum of the prepared MXene/SnO_2 nanocomposites were also performed as given in Figure 4, which confirms presence of SnO_2 nanoparticles onto the MXene surface. In our experimental conditions, we have successfully attached nanosized SnO_2 nanoparticles onto the MXene surface without altering the chemical composition and structure of MXene compared with previous reports.[31]

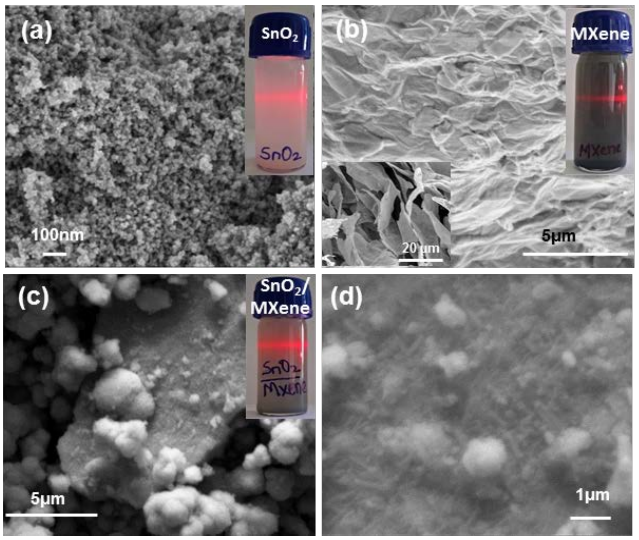

Figure 3. FESEM images of (a) SnO_2 nanoparticle, (b) few-layer MXene sheet, and (c and d) SnO_2/MXene nanostructures at different magnification. Inset images of each panel shows dispersion of pristine and composited nanostructures.

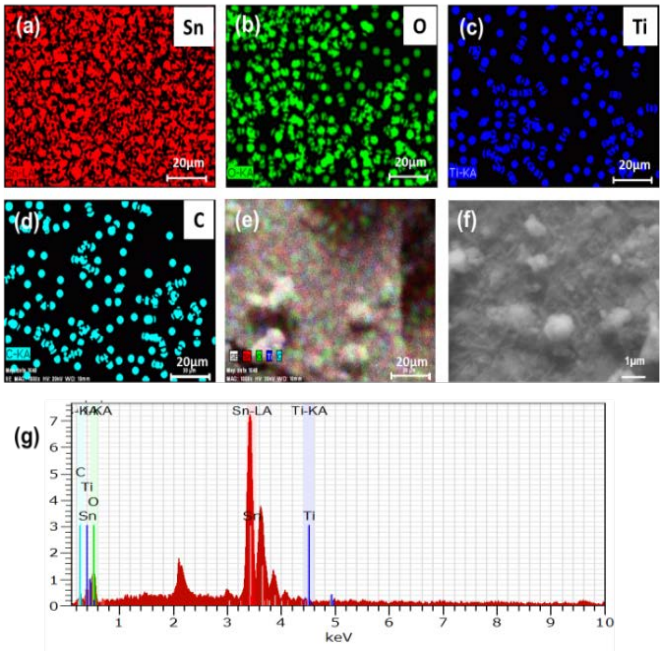

Figure 4. (a-f) Elemental compositional analysis, and (g) EDS spectrum of SnO_2/MXene nanocomposite.

Initially, gas sensing response of the SnO_2, MXene and SnO_2/MXene nanostructures has been analyzed using in-house fabricated gas sensing setup (Figure 1) for different ammonia gas concentration from 10 to 100 ppm as given in Figure 5a.

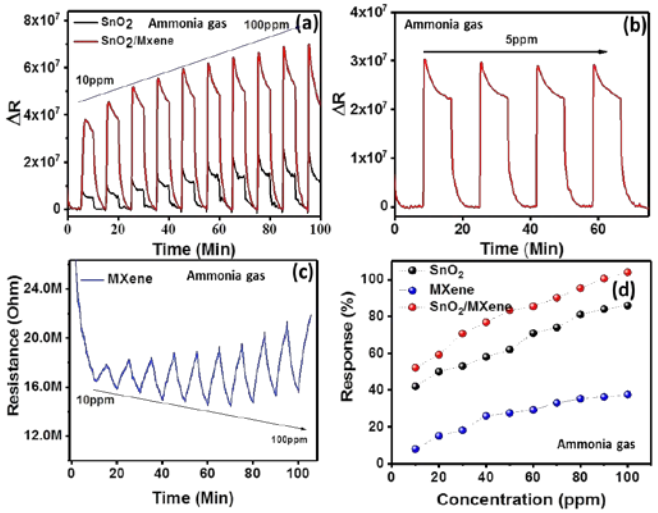

Figure 5. (a) Ammonia gas sensing performance of pristine SnO_2 and SnO_2/MXene from 10 to 100 ppm, (b) Reversibility and repeatability towards ammonia gas sensing performance of SnO_2/MXene tested at 5 ppm concentration, (c) Sensing performance of pristine MXene from 10 to 100 ppm of ammonia gas, and (d) Ammonia sensing response of SnO_2, MXene and SnO_2/MXene nanocomposite

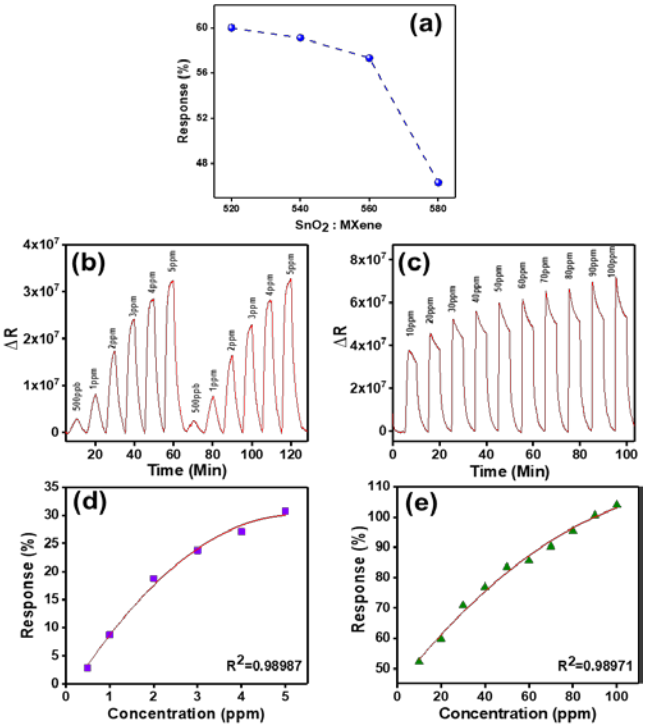

Figure 6. (a) Gas sensing response of different weight percentage of MXene loaded into SnO_2/MXene nanocomposites. Gas sensing performance of SnO_2/MXene nanocomposites at different tested ammonia concentrations (b) 500 ppb (part per billion) to 5 ppm, (c) 10 to 100 ppm, and (d and e) polynomial fit for gas sensing response of SnO_2/MXene nanocomposites.

The pristine SnO_2 samples shows increase in resistance when introducing different concentrations of ammonia gas molecules. Figure 5b shows the repeatability in gas sensing performance of fabricated MXene/SnO_2 nanocomposites at an ammonia gas of 5 ppm. However, the pristine MXene shows decrease in resistance upon exposing the ammonia vapors (Figure 5c). Here, gas sensing response was calculated by[32]

$$S\% = \frac{\Delta R}{Ra} \times 100$$

S is gas sensing response in percentage, $\Delta R = R_g - R_a$ (Resistance in gas and resistance in air). The gas sensing performance comparisons between the different fabricated samples are presented in Figure 5d. Remarkably, as supported from the Figure 5d the fabricated SnO_2/MXene nanocomposites show enhanced ammonia sensing performance compared to that of pristine MXene and SnO_2 nanoparticles. To further tune gas sensing performance by forming more heterojunction between SnO_2 and MXene, different weight percentage of MXene loaded SnO_2/MXene nanocomposites samples were prepared. The gas sensing performance of different MXene weight loaded SnO_2/MXene nanocomposites samples are presented in Figure 6a for ammonia for 10 ppm. It clearly shows that amount of MXene increases upon increasing the MXene loading. It is due to decrement of heterojunctions as expected.[33]

By loading more MXene layered structures onto the SnO_2 could possibly affects the active sites of metal oxide nanoparticles could diminish the gas sensing performance. Based on our experimental observation, we have selected 5mg of SnO_2 and 20µg of MXene is optimum composite fraction showing enhanced ammonia sensing performance. The gas sensing performance at fabricated SnO_2/MXene nanostructures were also analyzed at different (0.5-5ppm, and 10-100 ppm) concentrations. The results of different gas sensing performance of tested concentrations are shown in Figure 6a. As supported from the Figure 6(b and c), the increase in device resistance by increasing the ammonic gas concentrations. And, the fabricated SnO_2/MXene nanocomposites shows good polynomial fit R^2=0.98987, and 0.98971 for 0.5 - 10 ppm and 10 - 100 ppm, respectively which explicates that at higher ammonia dosage concentrations fabricated gas sensor attained saturation level. The estimated limit of detection (LOD) of fabricated the SnO_2/MXene nanocomposites using general expression[34] and is about 3.14 ppb. The response and recovery times of pristine SnO_2, MXene and SnO_2/MXene nanocomposites were calculated for 5 ppm ammonia gas concentration and results were presented in Figure 7. Compared to all naked nanostructures, the fabricated SnO_2/MXene nanostructures shows exemplary response time of about 16 s. Besides, bare SnO_2 nanoparticles and SnO_2/MXene nanostructures shows almost similar recovery time 77 and 86 s respectively. Gas selectivity is one of the primary evaluation steps to analyze the gas sensing characteristics of any fabricated gas sensors. Figure 8 (a and b) shows selectivity graph for SnO_2/MXene for different tested gas molecules. As evidenced from the Figure 8a, the lesser change in resistance were observed under exposure of various gas molecules such as formaldehyde, dimethylformamide, octane, toluene, acetone, methanol, ethanol at 2000 ppm concentration. Interestingly, fabricated

SnO_2/MXene based gas sensor device displayed remarkable change in resistance under exposure of ammonia gas at 100 ppm. The selective analysis in terms of gas sensing response was also plotted as given in Figure 8b. It reveals that the fabricated sensor was more selective towards target ammonia gas even at higher concentrations of interference gas molecules.

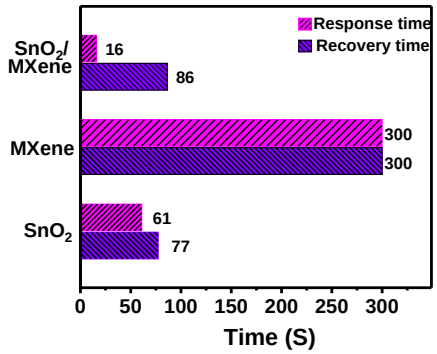

Figure 7. Response/Recovery time for pristine and SnO_2/MXene nanocomposites measured from 10 independent measurements under 5 ppm of ammonia.

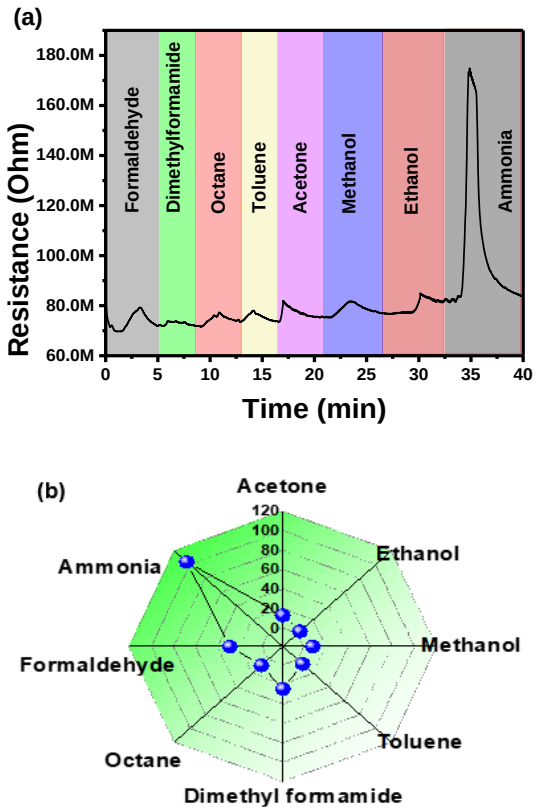

Figure 8. (a) Change in resistance of SnO_2/MXene sensor device under exposure of different gas molecules, and (b) Gas sensing response (%) of fabricated SnO_2/MXene for different gas molecules.

The vapor sensing mechanism of SnO_2/MXene is not clearly understood and call for further detailed investigations. Generally, the resistance of a n-type semiconductor sensor supposed to decrease while interacting with the reducing gas such as ammonia.[35] However, in the present case both SnO_2 and SnO_2/MXene found to exhibit anomalous behavior as their resistance found to increase upon exposed to reducing gas vapor (ammonia). Similar anomalous behavior of SnO_2 sensors were reported before.[31]

Conclusion

SnO_2 nanoparticles and MXene were synthesized separately and SnO_2/MXene nanocomposites were electrostatically assembled by ultra-sonication method. The SnO_2/MXene nanocomposites exhibited superior performance towards ammonia sensing compared to that of pristine SnO_2 and MXene sensors. SnO_2/MXene nanocomposite showed improved adsorption and desorption property as the response and recovery time was 16 s and 86 s respectively compared to the pristine SnO_2 showed slower response and recovery time of 61 s and 77 s. SnO_2/MXene nanocomposite was highly selective to ammonia sensing.

Acknowledgments

The author R. T. R thanks DST-SERB (No.EMR/2017/000300) for the financial support. The author acknowledges UGC-IUAC for the award of a Junior Research Fellow (IUAC/XIII.7/UFR-64312).

Conflict of Interest

Authors declared no conflict of interest.

References and Notes

1. M. Sathish, B. Madhan, P. Saravanan, J. Raghava Rao, B.U. Nair. Dry ice - An eco-friendly alternative for ammonium reduction in leather manufacturing. *J. Cleaner Produc.* **2013**, 54, 289–295.
2. A. Chiumenti, F. da Borso, A. Pezzuolo, L. Sartori, R. Chiumenti. Ammonia and greenhouse gas emissions from slatted dairy barn floors cleaned by robotic scrapers. *Res. Agricultural Engin.* **2018**, 64 (1), 26–33.
3. M. Ulbricht, J. Schneider, M. Stasiak, A. Sengupta. Ammonia recovery from industrial wastewater by trans Membrane chemiSorption. *Chemie-Ingenieur-Technik* **2013**, 85 (8), 1259–1262.
4. N.S. Nur, R. Yunus, C.F. Ishak, S. Hanif Khan. Laboratory Evaluation on Ammonia Volatilization from Coated Urea Fertilizers. *Commun. Soil Sci. Plant Analysis* **2018**, 49 (6), 717–724.
5. M. Mahdinia, S.H. Adeli, A. Mohammadbeigi, et al. Respiratory Disorders Resulting From Exposure to Low Concentrations of Ammonia: A 5-Year Historical Cohort Study. *J. Occupational Environ. Med.* **2020**, 62 (8), e431–e435.
6. L. Vatandoust, A. Habibi, H. Naghshara, S.M. Aref. Fabrication of ZnO-MWCNT nanocomposite sensor and investigation of its ammonia gas sensing properties at room temperature. *Synthetic Metals* **2021**, 273, 116710.
7. S.B. Jagadale, V.L. Patil, S.A. Vanalakar, P.S. Patil, H.P. Deshmukh. Preparation, characterization of 1D ZnO nanorods and their gas sensing properties. *Ceramics Int.* **2018**, 44 (3), 3333–3340.
8. S. Yuan, H. Ren, G. Meng, et al. ZnO monolayer supported single atom catalysts for efficient nitrogen electroreduction to ammonia. *Appl. Surface Sci.* **2021**, 555, 149682.
9. D. Punetha, S.K. Pandey. Enhancement and Optimization in Sensing Characteristics of Ammonia Gas Sensor Based on Light Assisted Nanostructured WO3Thin Film. *IEEE Sensors J.* **2020**, 20 (24), 14617–14623.
10. V.T. Duong, C.T. Nguyen, H.B. Luong, D.C. Nguyen, H.L. Nguyen. Ultralow-detection limit ammonia gas sensors at room temperature

based on MWCNT/WO3 nanocomposite and effect of humidity. *Solid State Sciences* **2021**, 113, 106534.
11. H. Fu, Q. Wang, J. Ding, et al. Fe2O3 nanotube coating micro-fiber interferometer for ammonia detection. *Sensors and Actuators, B: Chemical* **2020**, 303, 127186.
12. L. Bigiani, D. Zappa, C. Maccato, et al. Mn3O4 Nanomaterials Functionalized with Fe2O3 and ZnO: Fabrication, Characterization, and Ammonia Sensing Properties. *Advanced Materials Interfaces* **2019**, 6 (24), 1901239.
13. N. Sakhuja, R. Jha, N. Bhat. Facile green synthesis of 2D hexagonal MoO3 for selective detection of ammonia at room temperature. *Materials Science and Engineering B: Solid-State Materials for Advanced Technology* **2021**, 271, 115249.
14. T. Thomas, N. Jayababu, J. Shruthi, et al. Room temperature ammonia sensing of α-MoO3 nanorods grown on glass substrates. *Thin Solid Films* **2021**, 722, 138575.
15. R. Ghosh, A. Midya, S. Santra, S.K. Ray, P.K. Guha. Chemically reduced graphene oxide for ammonia detection at room temperature. *ACS Applied Materials and Interfaces* **2013**, 5 (15), 7599–7603.
16. A. Bag, D. bin Moon, K.H. Park, C.Y. Cho, N.E. Lee. Room-temperature-operated fast and reversible vertical-heterostructure-diode gas sensor composed of reduced graphene oxide and AlGaN/GaN. *Sensors and Actuators, B: Chemical* **2019**, 296, 126684.
17. N. Sakhuja, R. Jha, N. Bhat. Facile green synthesis of 2D hexagonal MoO3 for selective detection of ammonia at room temperature. *Mater. Sci. Engin. B: Solid-State Mater. Adv. Technol.* **2021**, 271, 115249.
18. E. Lee, D.-J. Kim. Review- Recent Exploration of Two-Dimensional MXenes for Gas Sensing: From a Theoretical to an Experimental View. *J. Electrochem. Soc.* **2020**, 167 (3), 037515.
19. E. Lee, A. Vahidmohammadi, Y.S. Yoon, M. Beidaghi, D.J. Kim. Two-dimensional vanadium carbide mxene for gas sensors with ultrahigh sensitivity toward nonpolar gases. *ACS Sensors* **2019**, 4 (6), 1603–1611.
20. N. Kumar, K. Navin, R.J. Ball, R. Kurchania. Mechanical and structural properties of aluminium nanocomposites reinforced with cerium oxide nanoparticles fabricated by powder metallurgy. *J. Mater. NanoSci.* **2020**, 7(2), 73-78.
21. Z. Wang, F. Wang, A. Hermawan, et al. SnO-SnO2 modified two-dimensional MXene Ti3C2Tx for acetone gas sensor working at room temperature. *J. Mater. Sci. Technol.* **2021**, 73, 128–138.
22. S.A. Vanalakar, V.L. Patil, N.S. Harale, et al. Controlled growth of ZnO nanorod arrays via wet chemical route for NO2 gas sensor applications. *Sensors and Actuators, B: Chemical* **2015**, 221, 1195–1201.
23. Z. Şahin, R. Meunier-Prest, F. Dumoulin, et al. Tuning of organic heterojunction conductivity by the substituents' electronic effects in phthalocyanines for ambipolar gas sensors. *Sensors and Actuators, B: Chemical* **2021**, 332, 129505.
24. C. Cheng, H. Zhang, F. Li, S. Yu, Y. Chen. High performance ammonia gas detection based on TiO2/WO3·H2O heterojunction sensor. *Mater. Chem. Phys.* **2021**, 273, 125098.
25. J. Zhang, D. Leng, G. Li, et al. Bimetallic–organic framework-derived Co3O4–ZnO heterojunction nanofibers: A new kind of emerging porous nanomaterial for enhanced ethanol sensing. *Sensors and Actuators B: Chemical* **2021**, 349, 130732.
26. F. Wang, Z. Wang, J. Zhu, et al. Facile synthesis SnO2 nanoparticle-modified Ti3C2 MXene nanocomposites for enhanced lithium storage application. *J. Mater. Sci.* **2017**, 52 (7), 3556–3565.
27. K. Rajavel, X. Yu, P. Zhu, et al. Exfoliation and Defect Control of Two-Dimensional Few-Layer MXene Ti3C2T xfor Electromagnetic Interference Shielding Coatings. *ACS Appl. Mater. Interfaces* **2020**, 12 (44), 49737–49747.
28. R.K. Selvan, I. Perelshtein, N. Perkas, A. Gedanken. Synthesis of hexagonal-shaped SnO2 nanocrystals and SnO 2@C nanocomposites for electrochemical redox supercapacitors. *J. Physical Chem. C* **2008**, 112 (6), 1825–1830.
29. J. Xu, Q. Pan, an Shun, Z. Tian. Grain size control and gas sensing properties of ZnO gas sensor. *Sensors and Actuators B: Chemical*, **2000**, 66(1-3), 277-279.
30. Z. Song, J. Zhang, Y. Wang, J. Li. Influence of Li doping on the morphological evolution and optical & electrical properties of SnO2 nanomaterials and SnO2/Li2SnO3 composite nanomaterials. *Ceramics Int.* **2021**, 47 (17), 23821–23826.
31. A. Beniwal, V. Srivastava, Sunny. Sol-gel assisted nano-structured SnO2 sensor for low concentration ammonia detection at room temperature. *Mater. Res. Express* **2019**, 6 (4), 046421.
32. J.H. Lee. Technological realization of semiconducting metal oxide-based gas sensors. In *Gas Sensors Based on Conducting Metal Oxides: Basic Understanding, Technology and Applications*; Elsevier, **2018**; pp 167–216.
33. Y.G. Song, J.Y. Park, J.M. Suh, et al. Heterojunction Based on Rh-Decorated WO3 Nanorods for Morphological Change and Gas Sensor Application Using the Transition Effect. *Chem. Mater.* **2019**, 31 (1), 207–215.
34. J. Burgués, J.M. Jiménez-Soto, S. Marco. Estimation of the limit of detection in semiconductor gas sensors through linearized calibration models. *Analytica Chimica Acta* **2018**, 1013, 13–25.
35. S. Singh, R.M. Sattigeri, S. Kumar, P.K. Jha, S. Sharma. Superior Room-Temperature Ammonia Sensing Using a Hydrothermally Synthesized MoS2/SnO2Composite. *ACS Omega* **2021**, 6 (17), 11602–11613.